Journal of Thermal Analysis and Calorimetry, Vol. 81 (2005) 595–601

A COMPARATIVE STUDY OF THE EFFECTS OF DECOMPOSITION RATE CONTROL AND MECHANICAL GRINDING ON THE THERMAL DECOMPOSITION OF ALUMINUM HYDROXIDE

N. Koga[*]

Chemistry Laboratory, Department of Science Education, Graduate School of Education, Hiroshima University, 1-1-1 Kagamiyama, Higashi-Hiroshima 739-8524, Japan

Two different processes of the thermal decomposition of synthetic bayerite, i.e., the non-isothermal decomposition of mechanically ground sample in flowing N_2 and the controlled rate thermal decomposition of crystalline bayerite under vacuum, were investigated comparatively. In comparison with the conventional non-isothermal decomposition of crystalline bayerite in flowing N_2, the reaction temperature of the thermal decomposition was lowered by the individual effects of mechanical grinding of the sample and the reaction rate control. These decomposition processes indicated similar behavior characterized by the restricted changes of the specific surface area during the course of decomposition reaction and the formation of an amorphous alumina as the decomposition product. Different thermal behaviors were observed for those amorphous Al_2O_3 produced by the respective decomposition processes.

Keywords: *amorphous aluminum oxide, controlled rate thermal analysis, mechanochemical effect, synthetic bayerite, thermal decomposition*

Introduction

Because the kinetic behavior and the properties of the solid products of the thermal decomposition of solids are influenced largely by the reaction atmosphere applied and generated by the reaction itself [1, 2], precise control of the reaction atmosphere including the self-generated reaction condition is desired for the material synthesis through the thermal decomposition processes. Application of the principle of controlled rate thermal analysis (CRTA) [3–5] to the material synthesis through the thermal decomposition processes is one of the possible solutions to control the reaction atmosphere including the self-generated atmosphere, where the reaction atmosphere during the whole course of the reaction can be regulated precisely by controlling the decomposition rate. Effects of the decomposition rate control on the kinetic behaviors and the properties of the solid products have been examined as exemplified by various processes of thermal decomposition [5–15], providing fundamental understandings on the usefulness of the CRTA as an intelligent tool for controlling the process of material synthesis.

In our previous work [15], we have examined the effect of decomposition rate control under vacuum on the reaction pathway of the thermal decomposition of synthetic bayerite, β-$Al(OH)_3$. The decomposition process was characterized by the lowered reaction temperature and a very limited change of the specific surface area during the course of reaction, producing an amorphous alumina as the decomposition product. It was found that those observations are very similar to the reported reaction behavior of the non-isothermal decomposition of amorphous aluminum hydroxide obtained by the mechanical grinding of the crystalline bayerite [16]. A comparative study of the effects of decomposition rate control under vacuum and mechanical grinding of the sample on the reaction pathway and kinetic behavior of the thermal decomposition processes was carried out in the present work, in order to clarify the reasons for the similarities of the respective effects on the decomposition processes. The thermal behaviors of the amorphous alumina produced by the respective decomposition processes were also compared.

Experimental

Sample preparation

Aluminum hydroxide was prepared by the procedure reported previously [17]. Carbon dioxide was introduced, at a rate of 100 cm^3 min^{-1}, into 0.9 M sodium aluminate solution at room temperature until the pH value of the solution being down to 12.3. The precipitate produced during the carbonation process was aged in mother solution with mechanical stirring for 12 h. The precipitate was filtered and washed with

* nkoga@hiroshima-u.ac.jp

1388–6150/$20.00

Akadémiai Kiadó, Budapest, Hungary
Springer, Dordrecht, The Netherlands

water, and dried in vacuum desiccator. The precipitate was identified, as $Al(OH)_3$ with crystal structure of bayerite, by chemical analysis for Al^{3+}, FTIR spectroscopy, powder X-ray diffraction (XRD) and TG-DTA.

Controlled rate decomposition

The sample was weighed into an alumina boat (30 mm in length, 6 mm in width, and 4 mm in depth) and was sat in a tube furnace. The pressure in the tube furnace was reduced to $1.0 \cdot 10^{-3}$ Pa by diffusion and rotary pumps. Using an instrument of controlled rate evolved gas detection (CREGD) [15], the sample was heated up to 775 K by controlling the sample temperature so as to maintain the pressure to be $7.0 \cdot 10^{-3}$ Pa during the course of thermal decomposition.

Mechanical grinding

Mechanical grinding of the sample was carried out in line with the procedure reported by Tsuchida and Ichikawa [16]. The sample of 5 g was weighed into an alumina jar of 45 cm^3, together with seven alumina balls of 12 mm in diameter. Using a planetary mill (Fritsch P-7), the sample was ground at a rotation speed of 700 rpm for 30 h, where every one hour the grinding was stopped to scrape the sample from the balls and jars. The ground sample indicated no distinguished XRD peak with the specific surface area of 35.8 $m^2\ g^{-1}$.

Measurements

Using an instrument of ULVAC DTG-9600, TG-DTA curves for the as-prepared crystalline bayerite and the ground sample were measured at a heating rate of 30 K min^{-1} under flowing N_2 (100 $cm^3\ min^{-1}$). The changes of the XRD patterns during the thermal decomposition of these samples and the subsequent phase changes of the decomposition products were traced by heating at a rate of 2 K min^{-1} using an instrument of high temperature XRD (Rigaku RINT2200; monochrome CuK_α, 40 kV, 20 mA). The specific surface areas of the samples decomposed partially by heating at a rate of 2 K min^{-1} in flowing N_2 (100 $cm^3\ min^{-1}$) were measured by the single point method of BET using FlowSorbII-2300 (Micromeritics). DSC measurements for the decomposition products, obtained through the non-isothermal decomposition of ground sample in flowing N_2 and controlled rate thermal decomposition of crystalline bayerite under vacuum by heating up to 775 K, were carried out using a Rigaku DSC8160 at various heating rates under flowing N_2 (50 $cm^3\ min^{-1}$).

Results and discussion

Thermal decompisition processes

Figure 1 shows typical traces of reaction temperature and residual pressure during the controlled rate thermal decomposition of synthetic bayerite under vacuum. Initiating the decomposition reaction, the residual pressure in the reaction atmosphere increased due to the evolution of water vapor as the gaseous product. Through a feedback control of the reaction temperature by monitoring the residual pressure, the residual pressure during the course of reaction is controlled successfully at a constant value of $7 \cdot 10^{-3}$ Pa. At the end of the reaction, the reaction temperature increases rapidly to

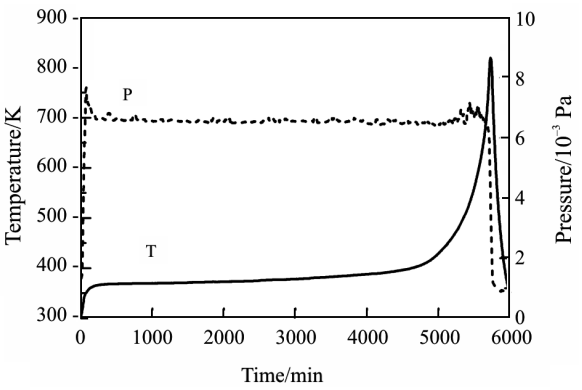

Fig. 1 Typical traces of reaction temperature and residual pressure during the controlled rate thermal decomposition of crystalline bayerite (300 mg) at a controlled pressure of 7.0 10^{-3} Pa

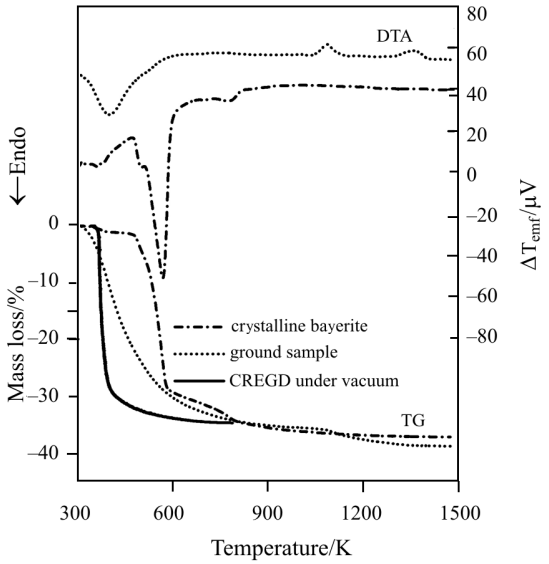

Fig. 2 Typical TG-DTA curves for the non-isothermal decompositions of crystalline bayerite and mechanically ground sample (ca. 20 mg), together with the reaction temperature of controlled rate thermal decomposition of synthetic bayerite (300 mg) by CREGD at a controlled pressure of 7.0 10^{-3} Pa

the limit temperature of measurement and the residual pressure decreases to the basal pressure of $1 \cdot 10^{-3}$ Pa. Because only water vapor is evolved through the present reaction as the gaseous product, the evolution rate of water vapor is also regulated at a constant rate. It has already been reported in our previous study [15] that an amorphous Al_2O_3 is produced as the decomposition product of the conrolled rate thermal decomposition of synthetic bayerite under vacuum.

Figure 2 compares TG-DTA curves for the thermal decompositions of crystalline bayerite and ground sample. As has been reported previously [17], the thermal decomposition of crystalline bayerite initiates at around 450 K and proceeds in two distinguished reaction steps via an intermediate product at around 600 K. The gradual mass loss is observed until 950 K. On the other hand, the thermal decomposition of ground sample takes place in a wide temperature range from room temperature to 950 K with smooth mass-loss trace and a broad endothermic DTA peak. At the higher temperature region, i.e., >950 K, the decomposition products indicate apparently different thermal behaviors. The synthetic bayerite indicate no distinguished thermal effect in the DTA curve at the higher temperature region. As for the ground sample, two exothermic DTA peaks are observed at around 1100 and 1350 K. Unexpectedly, apparent mass loss is observed at the temperature range between these two exothermic DTA peaks. By the first identification of the evolved gases at this stage by means of TG-MS, only water vapor was detected during the temperature region. The similar mass-loss behavior of the ground bayerite at the same temperature region has also been reported by Tsuchida and Ichikawa [16]. For a comparison, the trace of reaction temperature measured by CREGD under vacuum was also shown in Fig. 2. The controlled rate decomposition of synthetic bayerite under vacuum takes place at the lower temperature region from 370 to 600 K, even comparing with that for the thermal decomposition of the ground sample under linear heating. The respective influences of the lowered reaction temperature, induced by the mechanical grinding and controlled rate decomposition under vacuum, on the decomposition kinetics and the thermal behavior of the decomposition products were compared throughout the present study.

Figure 3 compares the changes of the XRD patterns during heating the synthetic bayerite and ground sample, together with those for the decomposition product of controlled rate decomposition under vacuum (heated up to 775 K). The crystalline bayerite decomposed in two distinguished reaction steps via the intermediate compound of boehmite AlO(OH) producing finally η-Al_2O_3 at around 950 K [17]. As for the amorphous $Al(OH)_3$ of ground sample, no distinguished XRD peak can be found at the early stage of decomposition until 500 K, where the decomposition reaction is already achieved to the fractional conversion of ca. 85%. At the higher temperature region corresponding to the temperature range of non-isothermal decomposition of crystalline bayerite, i.e. 500–900 K, a slight but detectable diffraction peak of η-Al_2O_3 at 45.7° can be observed. Accordingly, the decomposition product of amorphous $Al(OH)_3$ at 950 K is assumed as the amorphous Al_2O_3 mixed partially with poorly crystalline η-Al_2O_3. It has been reported [15] that, through the controlled rate decomposition of crystalline bayerite under vacuum, the diffraction peaks ascribed to β-$Al(OH)_3$ decrease the intensities monotonously without indicating any other diffraction peaks of crystalline product, as can be seen from the XRD pattern in Fig. 3c at 775 K.

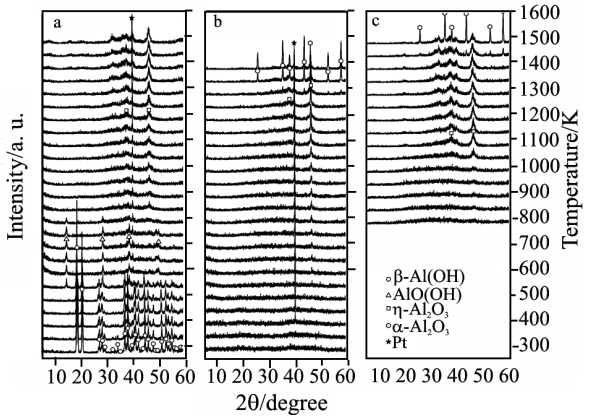

Fig. 3 Changes of XRD patterns during heating a – crystalline bayerite, b – ground sample, and c – amorphous decomposition product obtained by the controlled rate thermal decomposition of bayerite

Variations in the specific surface areas of the samples during the thermal decomposition were compared in Fig. 4. During the non-isothermal decomposition of

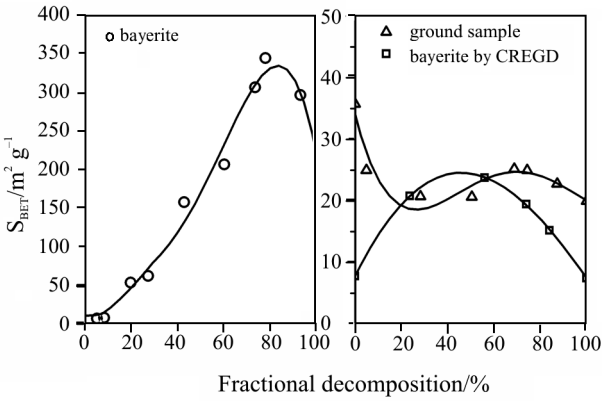

Fig. 4 Changes of specific surface area during the non-isothermal decompositions of crystalline bayerite and its ground sample in flowing N_2 and during the controlled rate thermal decomposition of crystalline bayerite at a controlled pressure of 7.0 10^{-3} Pa

crystalline bayerite, the specific surface area increases as reaction proceeds and indicates a maximum at around the fractional decomposition of 80%, which corresponds to the formation of intermediate product, AlO(OH). The remarkable increase in the specific surface area during the thermal decomposition has been explained by the formations of micropores of the product [16]. In contrast, no distinguished variation of the specific surface area can be observed during the thermal decomposition of ground sample, i.e., amorphous $Al(OH)_3$. The similar behavior can be seen for the controlled rate thermal decomposition of crystalline bayerite under vacuum. Two different interpretations of the phenomena have been made from the view points of a mechanochemical effect and a significant feature of the controlled rate decomposition under vacuum. From a mechanochemical viewpoint, Tsuchida and Ichikawa [16] assumed a probable facilitation of sintering during the course of decomposition even at the lowered reaction temperature due to the energies accumulated by the sample during grinding. As for the identical phenomena observed for the controlled rate thermal decomposition of crystalline gibbsite, α-$Al(OH)_3$, under vacuum, Rouquerol and Ganteaume [6] gave an interpretation concerning the mechanism of micropore formation during the thermal decomposition where the final micropore diameter depends on the mobilities of the Al^{3+} and H^+ ions. Because the mobilities of these ions at the reaction interface decrease by lowering the reaction temperature, size of the micropore is expected to be reduced under the controlled rate thermal decomposition in vacuum. The latter interpretation is also account for the phenomena observed for the thermal decomposition of ground sample, because the mobilities of the ions at the reaction interface seems to be decreased with the lowered reaction temperature.

Decomposition kinetics

For characterizing the apparent kinetic behaviors of the thermal decomposition processes, the respective series of kinetic rate data for the non-isothermal decomposition of ground sample in flowing N_2 and for the controlled rate thermal decomposition of crystalline bayerite under vacuum were collected. Figure 5 shows a series of kinetic rate data for the non-isothermal decomposition of ground sample under flowing N_2 at various heating rates. As shown in Fig. 6, a series of the kinetic rate data for the controlled rate thermal decomposition of crystalline bayerite under vacuum were measured by changing the sample masses under the conditions otherwise identical, i.e., basal pressure of $1.0 \cdot 10^{-3}$ Pa and controlled pressure of $7.0 \cdot 10^{-3}$ Pa. The value of apparent activation energy E_a at a selected fractional reaction α was calculated

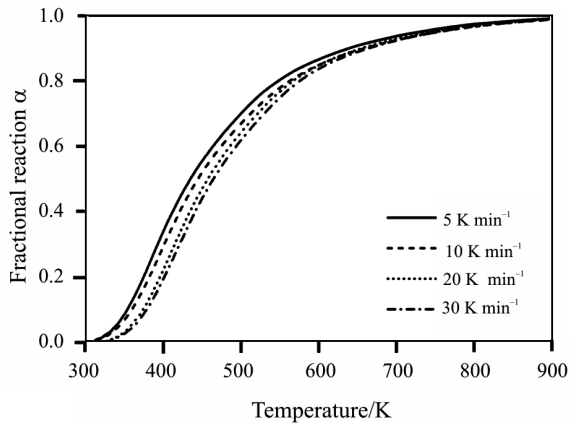

Fig. 5 A series of kinetic rate data measured at different heating rates for the non-isothermal decomposition of ground sample in flowing N_2

by Friedman method [18–20], according to the following equation.

$$\ln\left(\frac{d\alpha}{dt}\right) = \ln[Af(\alpha)] - \frac{E_a}{RT} \quad (1)$$

where A and $f(\alpha)$ is the pre-exponential factor of the Arrhenius equation and the kinetic model function in differential form. Other symbols have their usual meanings. By plotting $\ln(d\alpha/dt)$ *vs.* reciprocal temperature T^{-1} using the data points read from the series of kinetic rate data at a selected α, the value of E_a is evaluated from the slope of the Friedman plot. Figure 7 shows the values of E_a at various α. Quite different behaviors of the α-dependences of E_a values were observed between the processes under comparison. The E_a values for the controlled rate thermal decomposition of crystalline bayerite under vacuum indicate a constant value of 44±2 kJ mol^{-1} in a wide range of reaction, $0.05 \leq \alpha \leq 0.80$. By contrast, for the non-isothermal decomposition of ground sample in flowing

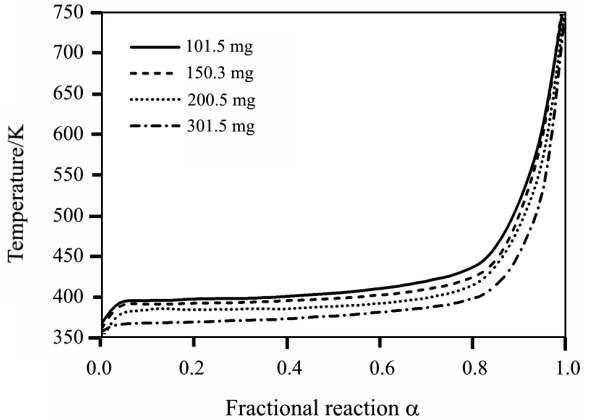

Fig. 6 A series of kinetic rate data measured using different sample masses for the controlled rate decomposition of crystalline bayerite at a controlled pressure of $7.0\ 10^{-3}$ Pa

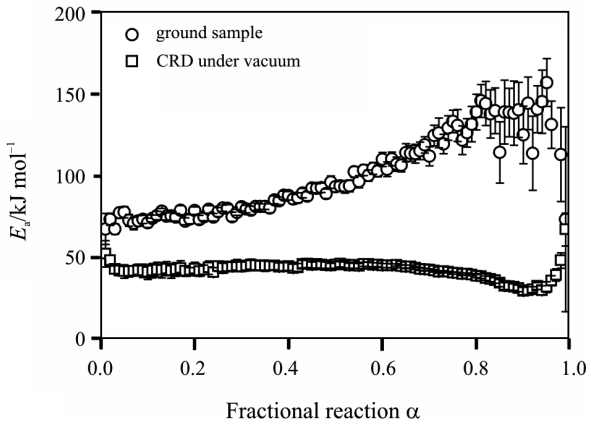

Fig. 7 Apparent values of E_a at different α evaluated for the non-isothermal decomposition of ground sample in flowing N_2 and for the controlled rate decomposition (CRD) of crystalline bayerite at a controlled pressure of 7.0 10^{-3} Pa

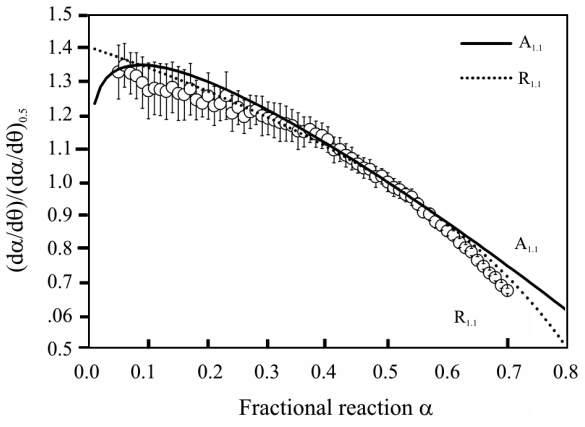

Fig. 8 The experimental master plot of $(d\alpha/d\theta)/(d\alpha/d\theta)_{0.5}$ *vs.* α for the controlled rate decomposition of crystalline bayerite under vacuum, together with theoretical master plots drawn by assuming the $R_{1.1}$ and $A_{1.1}$ laws

N_2, the E_a values increase gradually from about 70 to 140 kJ mol^{-1} as reaction advances. The observed variation of the E_a values during the course of non-isothermal decomposition of ground sample implies the possible change of the reaction mechanism depending on the reaction temperature distributed widely from room temperature to 950 K. It has been shown by ^{27}Al MASS NMR for the effect of mechanical grinding of gibbsite [21] that the originally octahedral coordination structure of aluminum ions and layered structure of hydroxyl groups are destructed by the mechanical grinding by showing partially the lower coordination in aluminum ions, i.e., tetrahedral and 5-fold coordination structures. Similar structural distribution induced by mechanical grinding, expected also in the ground sample of bayerite, accounts for the widened range of reaction temperature and systematic variation in the decomposition mechanism. Because direct application of the fundamental kinetic equation, based on an invariant reaction mechanism during the course of reaction, to such complicated process with systematic variation in the E_a values as reaction proceeds is not allowed, the further detailed kinetic characterization for the non-isothermal decomposition of ground sample in flowing N_2 was discouraged at present.

By taking the constant value of E_a observed in a wide range of α as the evidence of the applicability of the fundamental kinetic equation, a simulated kinetic curve at infinite temperature was drawn for the controlled rate thermal decomposition of crystalline bayerite in vacuum by assuming the following equation:

$$\frac{d\alpha}{d\theta} = \frac{d\alpha}{dt}\exp\left(\frac{E_a}{RT}\right) = Af(\alpha) \qquad (2)$$

where θ is the generalized time proposed originally by Ozawa [22]. Figure 8 shows the experimental master plot of simulated rate data at infinite temperature, $(d\alpha/d\theta)/(d\alpha/d\theta)_{0.5}$ *vs.* α [23, 24], for the controlled rate thermal decomposition of crystalline bayerite in vacuum. The experimental master curve is decelerating and convex slightly in the shape. According to Eq. 2, the apparent fitting of the formal kinetic model function was compared by plotting $d\alpha/d\theta$ *vs.* various $f(\alpha)$. Rather good linear fittings were observed when using an Avrami-Erofeev law (A_m), $f(\alpha) = m(1-\alpha)[-\ln(1-\alpha)]^{1-1/m}$ with m=1.1, and a phase boundary controlled law (R_n), $f(\alpha)=n(1-\alpha)^{1-1/n}$ with n=1.1, that correspond very closely to the first order and zero order equations, respectively. As was shown in Fig. 8, the apparent fitting to those rate laws can be confirmed by comparing the experimental master plot with the theoretical curves of $f(\alpha)/f(0.5)$ *vs.* α drawn by assuming $R_{1.1}$ and $A_{1.1}$ laws. The apparent values of A evaluated from the slopes of $(d\alpha/d\theta)$ *vs.* $f(\alpha)$ plots were 24.3 and 5.1 s^{-1} for the $R_{1.1}$ and $A_{1.1}$ laws, respectively.

Crystallization of amorphous alumina

Figure 9 compares typical DSC curves for the amorphous decomposition products obtained through the non-isothermal decomposition of ground sample in flowing N_2 and controlled rate thermal decomposition of crystalline bayerite under vacuum. Both the amorphous decomposition products indicate exothermic peaks at the same temperature range of 900–1150 K. By comparing with the changes of XRD patterns during heating the samples shown in Fig. 3, these exothermic peaks observed for both the samples are ascribed to the crystallization of η-Al_2O_3 from amorphous Al_2O_3. The enthalpy changes during the crystallization of η-Al_2O_3 differ largely between the dehydrated samples, i.e. –18.8±0.7 and –31.4±1.1 kJ (mol Al_2O_3)$^{-1}$ for the amorphous decomposition products obtained from the non-isothermal decomposition

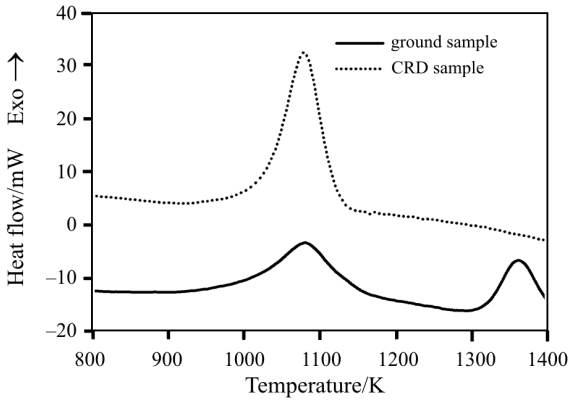

Fig. 9 Typical DSC traces for the amorphous decomposition products produced through the non-isothermal decomposition of the ground sample in flowing N_2 and the controlled rate decomposition (CRD) of crystalline bayerite under vacuum

of ground sample in flowing N_2 and controlled rate thermal decomposition of crystalline bayerite under vacuum, respectively. Partial crystallization of η-Al_2O_3 during the non-isothermal decomposition of ground sample is assigned to one of the reasons for the differences of the enthalpy changes.

On the basis of a series of DSC traces at different heating rates β, the apparent values of E_a for the overall crystallization processes were determined by the Kissinger plots [25] according to

$$\ln\frac{\beta}{T_p^2} = \ln\left(-f'(\alpha_p)\frac{AR}{E_a}\right) - \frac{E_a}{RT_p} \qquad (3)$$

where subscript *p* indicates the peak maximum. Because the logarithmic term in the right hand side of Eq. 3 can be approximated as constant, the value of E_a can be calculated from the slope of the plot of $\ln(\beta/T_p^2)$ *vs.* T_p^{-1}. Figure 10 compares the Kissinger plots for the overall crystallization processes of the amorphous decomposition products. It is apparent that the slopes of the Kissinger plots for the respective crystallization processes of η-Al_2O_3 are practically

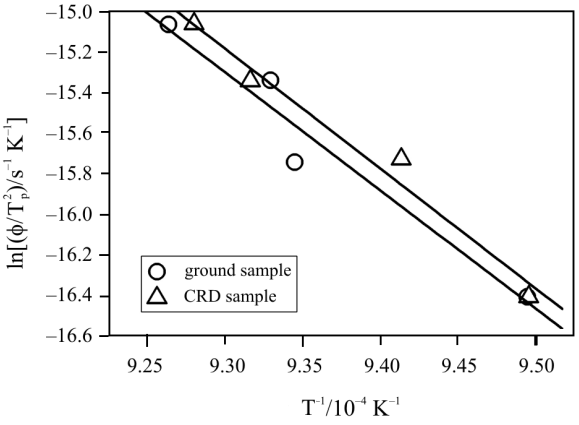

Fig. 10 The Kissinger plots for the crystallization of η-Al_2O_3

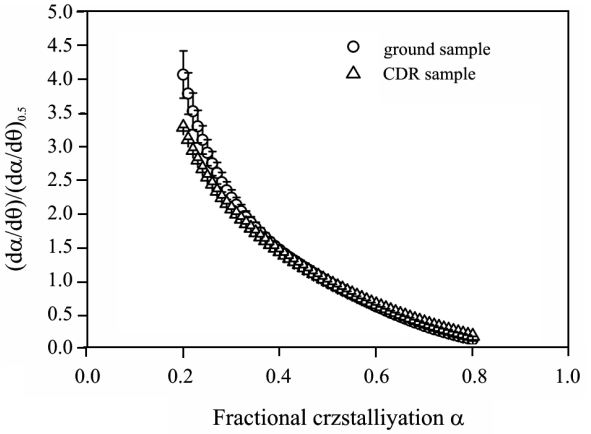

Fig. 11 The experimental master plot of $(d\alpha/d\theta)/(d\alpha/d\theta)_{0.5}$ *vs.* α for the crystallization process of η-Al_2O_3

identical. From the slope of the Kissinger plots, the values of E_a were calculated as 481±24 and 488±16 kJ mol^{-1} for the crystallization of amorphous decomposition products obtained from the non-isothermal decomposition of ground sample in flowing N_2 and controlled rate thermal decomposition of crystalline bayerite under vacuum, respectively. Using the values of E_a, experimental master curves, $(d\alpha/d\theta)/(d\alpha/d\theta)_{0.5}$ *vs.* α were drawn as shown in Fig. 11. Both the experimental master curves are concave in the shape, indicating the overall kinetic behavior controlled by diffusion of chemical species [23, 24].

Within the temperature region of the present DSC measurements, an alternative exothermic peak at the higher temperature was observed only for the decomposition product of the ground sample at around 1300–1400 K, Fig. 9. The secondary exothermic peak corresponds to the transformation of η-Al_2O_3 to α-Al_2O_3, as can be seen from the changes of XRD patterns shown in Fig. 3b. As for the decomposition product of controlled rate decomposition, the diffraction peaks of α-Al_2O_3 is observed at around 1475 K, Fig. 3c. Because the formation of α-Al_2O_3 during linear heating of crystalline bayerite can not be detected clearly even heating up to 1475 K, Fig. 3a, it is apparent that the formation temperature of α-Al_2O_3 is lowered by both the effects of mechanical grinding of the sample and the controlled rate decomposition under vacuum. As is deduced from the differences in the intensities and half-width of the diffraction peaks of η-Al_2O_3, the variation in the formation temperature of α-Al_2O_3 is likely due to the different crystallinities of η-Al_2O_3 produced through different reaction pathways.

Conclusions

The temperature range of the thermal decomposition of synthetic bayerite is apparently lowered by the re-

spective effects of mechanical grinding of the sample and the reaction rate control under vacuum. Both the decomposition processes, i.e. the non-isothermal decomposition of ground sample in flowing N_2 and the controlled rate thermal decomposition of crystalline bayerite under vacuum, are characterized by the very limited change of the specific surface area of the sample during the course of the thermal decomposition and by the formation of amorphous Al_2O_3 as the decomposition product. These decomposition processes, however, indicated different kinetic behaviors. The controlled rate decomposition of crystalline bayerite under vacuum was characterized kinetically by a monotonously decelerate process with the constant value of E_a=44±2 kJ mol^{-1}, whereas the values of E_a for the non-isothermal decomposition of ground sample increased gradually from 70 to 140 kJ mol^{-1} as reaction advances due to the possible variation of reaction mechanism.

The decomposition products, amorphous Al_2O_3, produced by the respective decomposition processes were crystallized to η-Al_2O_3 at around 900–1150 K, with a comparable kinetic behavior of diffusion controlled transformation with E_a≈480 kJ mol^{-1}. A difference is again appeared in the transformation temperature of η-Al_2O_3 to α-Al_2O_3, where the transformation of η-Al_2O_3 produced through heating the ground sample took place at the lower temperature by about 150 K.

References

1 A. K. Galway and M. E. Brown, Thermal Decomposition of Ionic Solids, Elsevier, Amsterdam 1999.
2 N. Koga and H. Tanaka, Thermochim. Acta, 288 (2002) 41.
3 J. Rouquerol, Thermochim. Acta, 144 (1989) 209.
4 J. Rouquerol, Thermochim. Acta, 300 (1997) 247.
5 O. T. Sørensen and J. Rouquerol, Sample Controlled Thermal Analysis, Kluwer, Dordrecht, 2003.
6 J. Rouquerol and M. Ganteaume, J. Thermal Anal., 11 (1977) 201.
7 N. Koga and J. M. Criado, Int. J. Chem. Kinet., 30 (1998) 737.
8 N. Koga, J. M. Criado and H. Tanaka, Thermochim. Acta, 340/341 (1999) 387.
9 L. A. Perez-Maqueda, J. M. Criado, C. Real, J. Šubrt and J. Bohacek, J. Mater. Chem., 9 (1999) 1839.
10 M. D. Alcala, F. J. Gotor, L. A. Perez-Maqueda, C. Real, M. J. Dianez and J. M. Criado, J. Therm. Anal. Cal., 56 (1999) 1447.
11 G. S. Chopra, C. Real, M. D. Alcala, L. A. Perez-Maqueda, J. Šubrt and J. M. Criado, Chem. Mater., 11 (1999) 1128.
12 N. Koga, J. M. Criado and H. Tanaka, J. Therm. Anal. Cal., 60 (2000) 943.
13 J. M. Criado, J. Therm. Anal. Cal., 72 (2003) 1097.
14 E. A. Fesenko, P. A. Barnes, G. M. B. Parkes, D. R. Brown and N. Naderi, J. Therm. Anal. Cal., 72 (2003) 1103.
15 N. Koga and S. Yamada, Solid State Ionics, 172 (2004) 253.
16 T. Tsuchida and N. Ichikawa, React. Solids, 7 (1989) 207.
17 N. Koga, T. Fukagawa and H. Tanaka, J. Therm. Anal. Cal., 64 (2001) 965.
18 H. L. Friedman, J. Polym. Sci., Part C, 6 (1964) 183.
19 T. Ozawa, J. Thermal Anal., 31 (1986) 547.
20 N. Koga, Thermochim. Acta, 258 (1995) 145.
21 K. J. D. MacKenzie, J. Temuujin and K. Okada, Thermochim. Acta, 327 (1999) 103.
22 T. Ozawa, Thermochim. Acta, 100 (1986) 109.
23 F. J. Gotor, J. M. Criado, J. Malek and N. Koga, J. Phys. Chem. A, 104 (2000) 10777.
24 J. M. Criado, L. A. Perez-Maqueda, F. J. Gotor, J. Malek and N. Koga, J. Therm. Anal. Cal., 72 (2003) 901.
25 H. E. Kissinger, Anal. Chem., 29 (1957) 1702.

DOI: 10.1007/s10973-005-7088-7